

## Article

# Contrasted Effect of Spinel and Pyroxene on Molecular Hydrogen (H<sub>2</sub>) Production during Serpentinization of Olivine

Ruifang Huang <sup>1,\*</sup>, Xing Ding <sup>2</sup>, Weidong Sun <sup>3,4</sup> and Xiuqi Shang <sup>3,4,5</sup>

- <sup>1</sup> SUSTech Academy for Advanced Interdisciplinary Studies, Southern University of Science and Technology, Shenzhen 518055, China
- <sup>2</sup> State Key Laboratory of Isotope Geochemistry, Guangzhou Institute of Geochemistry, Chinese Academy of Sciences, Guangzhou 510640, China; xding@gig.ac.cn
- <sup>3</sup> Center of Deep Sea Research, Institute of Oceanology, Chinese Academy of Sciences, Qingdao 266071, China; weidongsun@gig.ac.cn (W.S.); shangxq@qdio.ac.cn (X.S.)
- <sup>4</sup> Laboratory for Marine Mineral Resources, Qingdao National Laboratory for Marine Science and Technology, Qingdao 266237, China
- <sup>5</sup> Institute of Oceanology, University of Chinese Academy of Sciences, Beijing 100049, China
- \* Correspondence: huangrf@sustech.edu.cn

**Abstract:** Serpentinization produces molecular hydrogen (H<sub>2</sub>) and hydrocarbons that can feed the colonies of microbes in hydrothermal vent fields, and therefore serpentinization may be important for the origins of life. However, the mechanisms that control molecular hydrogen (H<sub>2</sub>) production during serpentinization remain poorly understood. Here the effect of pyroxene minerals and spinel on molecular hydrogen (H<sub>2</sub>) generation during serpentinization is experimentally studied at 311–500 °C and 3.0 kbar, where olivine, individually and in combinations with pyroxene and/or spinel, is reacted with saline solutions (0.5 M NaCl). The results show a contrasting influence of spinel and pyroxene on molecular hydrogen (H<sub>2</sub>) production. At 311 °C and 3.0 kbar, spinel promotes H<sub>2</sub> generation by around two times, and pyroxene minerals decrease molecular hydrogen (H<sub>2</sub>) production by around one order of magnitude. Spinel leaches aluminum (Al) and chromium (Cr) during hydrothermal alteration, and Al and Cr enhance molecular hydrogen (H<sub>2</sub>) production. This is confirmed by performing experiments on the serpentinization of olivine with the addition of Al<sub>2</sub>O<sub>3</sub> or Cr<sub>2</sub>O<sub>3</sub> powders, and an increase in molecular hydrogen (H<sub>2</sub>) production was observed. Pyroxene minerals, however, not only leach Al and Cr, but they also release silica (SiO<sub>2</sub>) during serpentinization. The sharp decline in molecular hydrogen (H<sub>2</sub>) production in experiments with a combination of olivine and pyroxene minerals may be attributed to releases of silica from pyroxene minerals. With increasing temperatures (e.g., 400–500 °C), the effect of spinel and pyroxene minerals on molecular hydrogen (H<sub>2</sub>) production is much less significant, which is possibly related to the sluggish kinetics of olivine serpentinization under these T-P conditions. In natural geological settings, olivine is commonly associated with spinel and pyroxene, and molecular hydrogen (H<sub>2</sub>) during serpentinization can be greatly affected.

**Keywords:** molecular hydrogen; serpentinization; spinel; pyroxene minerals



check for updates

**Citation:** Huang, R.; Ding, X.; Sun, W.; Shang, X. Contrasted Effect of Spinel and Pyroxene on Molecular Hydrogen (H<sub>2</sub>) Production during Serpentinization of Olivine. *Minerals* **2021**, *11*, 794. <https://doi.org/10.3390/min11080794>

Academic Editor: Shoji Arai

Received: 3 July 2021

Accepted: 19 July 2021

Published: 22 July 2021

**Publisher's Note:** MDPI stays neutral with regard to jurisdictional claims in published maps and institutional affiliations.



**Copyright:** © 2021 by the authors. Licensee MDPI, Basel, Switzerland. This article is an open access article distributed under the terms and conditions of the Creative Commons Attribution (CC BY) license (<https://creativecommons.org/licenses/by/4.0/>).

## 1. Introduction

Serpentinization is a hydrothermal alteration of ultramafic rocks at temperatures of ≤500 °C, and the reaction of olivine and pyroxene in ultramafic rocks with aqueous fluids results in the production of serpentine, (±) brucite, (±) talc and (±) magnetite. Mantle peridotites are abundantly exposed at mid-ocean ridges, and hydrothermal activity results in serpentinization of mantle peridotites. The presence of a serpentinite layer near the base of the mantle wedge has been indicated by geological and geophysical evidence [1–3]. Fluids associated with serpentinizing peridotites commonly contain abundant molecular hydrogen (H<sub>2</sub>) and hydrocarbons [4–7]. Molecular hydrogen (H<sub>2</sub>) and methane (CH<sub>4</sub>)

can feed the colonies of microbes from many geological settings, such as hydrothermal vents, alkaline springs, and the deep subsurface [8–12], indicating that serpentinization may be crucial for the genesis of life [13–17]. Occurrences of H<sub>2</sub>- and CH<sub>4</sub>-rich fluid inclusions derived from a harzburgite in subduction zones may be closely associated with serpentinization of peridotites in the mantle wedge [18], which may greatly influence oxygen fugacity of subduction zones.

Thermodynamic models and experiments have been performed to study molecular hydrogen (H<sub>2</sub>) production during serpentinization, mostly regarding the serpentinization of olivine [19–32]. Molecular hydrogen (H<sub>2</sub>) production was found to depend on many factors, including temperature, water/rock ratios, chemical compositions and pH of starting fluids [23,29,30,33,34]. The influence of other factors (e.g., pyroxene and spinel) on molecular hydrogen (H<sub>2</sub>) production, however, remains unclear. Our experimental studies suggest that the serpentinization of peridotite proceeds at faster rates compared to olivine hydrothermal alteration, resulting from the effect of pyroxene and spinel leaching aluminum and chromium [35,36]. The rates of reaction are directly linked to molecular hydrogen (H<sub>2</sub>) production during serpentinization [24], and therefore pyroxene and spinel may affect molecular hydrogen (H<sub>2</sub>) production.

In this study, we carried out serpentinization experiments at 311–500 °C and 3.0 kbar, and a combination of olivine, (±) spinel and (±) pyroxene minerals was reacted with saline solutions. The aims of this study are to (1) quantify the effect of spinel and pyroxene on molecular hydrogen (H<sub>2</sub>) production during olivine serpentinization, (2) investigate temperature dependence for the effect of spinel and pyroxene on molecular hydrogen (H<sub>2</sub>) formation, and (3) study the factors that control molecular hydrogen (H<sub>2</sub>) production during the serpentinization of olivine.

## 2. Materials and Methods

Olivine and spinel were chosen from a peridotite sample that occurs as xenoliths in basalts at Panshishan, Jiangsu Province, China [37–39]. Peridotite has been used in previous experiments [29,35,36]. Olivine and spinel were ground in an agate mortar and sieved into starting grain sizes of <30 μm, and they were cleaned in an ultrasonic water bath to remove fine particles. A combination of olivine and spinel/pyroxene was made. Saline solutions (0.5 M NaCl), the starting fluids of this study, were prepared with analytical reagent sodium chloride and deionized water.

The experiments were carried out in cold-sealed hydrothermal vessels [29,35,36]. Gold capsules with solid reactants and starting solutions (mass ratios of ~1.0) were welded at two sides and placed into hydrothermal vessels (Table 1). After experiments, the amounts of molecular hydrogen (H<sub>2</sub>) in the gold capsules were measured by using an Agilent 7890A gas chromatograph at the State Key Laboratory of Organic Geochemistry, Guangzhou Institute of Geochemistry, Guangzhou, China, with a detailed description of analytical procedures presented by several studies [40,41]. The solid run products were completely recovered, and the XRD patterns were collected utilizing a Rigaku Smartlab X-ray diffractometer in a high-pressure laboratory at the Southern University of Science and Technology, Guangzhou, China, with 2θ ranging from 10° to 90° at a step size of 0.02° and a counting time of 10 s per step. The morphology of the solid run products was observed using a Zeiss Ultra 55 field emission gun scanning electron microscope at 5 kV at the Second Institute of Oceanography, Ministry of Natural Resources, Hangzhou, China. The products were placed on a carbon tape, and they were subsequently coated with a thin platinum film. FTIR measurements (in transmission mode) were performed with a Bruker Vector–33 FTIR spectrometer at Analytical and Testing Center of South China University of Technology. Potassium bromide (KBr) pellets were prepared, and around 1 mg of sample was homogenized with 200 mg of KBr. The spectra were collected from 400 to 4000 cm<sup>−1</sup> at a resolution of 4 cm<sup>−1</sup>, with 32 scans for each spectrum.

Table 1. Experimental conditions.

Run no.	T (°C)	P (kbar)	Olivine (mg)	Solution (mg)	Spinel, Al <sub>2</sub> O <sub>3</sub> , Cr <sub>2</sub> O <sub>3</sub> (mg)	W/R Ratios	Time (Days)	H <sub>2</sub> (mmol/kg)	Reaction Extent (%) <sup>c</sup>
Olivine Only									
HR-16	311	3.0	50.7	50.9	—	1.0	13	100	69 (1.3)
HR-76	311	3.0	49.2	51.2	—	0.96	27	80	76 (1.7)
HR-106	311	3.0	49.3	50.2	—	1.0	10	95	62 (0.5)
Fe-57 <sup>a</sup>	400	3.5	35.9	46.7	—	1.3	19	0.83	0.5 (0.5)
Fe-46 <sup>a</sup>	535	3.6	65.7	101.7	—	1.5	18	2.2	0.0 (0.0)
Olivine + Al <sub>2</sub> O <sub>3</sub>									
HR-92	311	3.0	39.4	37.5	6.5	0.82	29	203	90 (0.7)
HR-94	311	3.0	50.0	50.9	12.7	0.95	27	132	—
HR-108	311	3.0	51.3	51.1	6.5	0.88	19	233	54 (3.8)
HR-72	505	3.0	36.2	37.9	11.8	0.79	20	3.7	0.5 (0.2)
Olivine + Cr <sub>2</sub> O <sub>3</sub>									
HR-95	311	3.0	49.4	50.9	6.3	0.91	27	166	77 (3.2)
HR-99	311	3.0	51.7	57.8	13.2	0.90	27	271	84 (2.8)
HR-109	311	3.0	52.0	50.4	6.7	0.86	18	268	54 (3.8)
Olivine + Spinel									
HR-84	200	3.1	32.7	28.7	7.1	0.72	13	1.5	0.4 (0.5)
HR-93	311	3.0	49.3	47.5	1.9	0.93	28	259	99 (0.9)
HR-75	311	3.0	49.7	51.4	6.6	0.92	27	260	100 (1.0)
HR-110	311	3.0	52.0	51.6	6.3	0.88	15	130	64 (0.6)
HR-73	505	3.0	36.4	36.7	12.8	0.75	20	5.7	0.5 (0.6)
Olivine + Pyroxene									
HR-88	311	3.0	30.7	27.8	—	0.90	27	15	100 (1.0)
HR-68	405	3.0	51.4	36.5	—	0.71	20	2.3	53 (3.5)
HR-70	505	3.0	20.1	19.6	—	0.97	19	6.3	5 (0.1)
HR-83 <sup>b</sup>	505	3.0	50.3	51.5	—	1.0	36	1.7	5 (0.3)
Spinel-Bearing Peridotite									
HR86	311	3.0	59.2	51.1	—	0.86	27	119	99 (1.7)
HR-69	405	3.0	54.2	41.2	—	0.76	20	16	99 (2.2)
HR-71	505	3.0	20.1	19.5	—	0.97	20	14	6 (0.1)

W/R ratios: ratios between the mass of a saline solution and solid reactants loaded into gold capsules. <sup>a</sup> Data from [27], olivine with starting grain sizes of 100–177 µm was used. <sup>b</sup> Peridotite with starting grain sizes of 100–177 µm was used. <sup>c</sup> The numbers in brackets are standard deviation of at least three times analyses.

### 3. Results and Discussion

#### 3.1. Characterization of Experimental Products

The conventional methods (X-ray diffraction, SEM and FTIR) revealed that the major hydrous phase in experimental products at 311 °C and 3.0 kbar was fibrous chrysotile except those using mechanical mixtures of olivine and ~12.0 mg Al<sub>2</sub>O<sub>3</sub> powders, where chlorite was produced (Figures 1 and 2). Serpentine formation is evidenced by infrared spectra with stretching modes at 954 cm<sup>-1</sup> and 3686 cm<sup>-1</sup> [42,43]. The band at 954 cm<sup>-1</sup> is attributed to the stretching mode of the Si-O group in serpentine, and the band at 3686 cm<sup>-1</sup> represents the stretching vibration of the -OH group in serpentine [42,43]. At 400 °C and 3.0 kbar, the dominant secondary hydrous phase was lizardite (Figure 2). Lizardite and talc were produced in experiments at 500 °C and 3.0 kbar, and talc formation is attested by its stretching modes at 671 cm<sup>-1</sup> and 3677 cm<sup>-1</sup> [44].

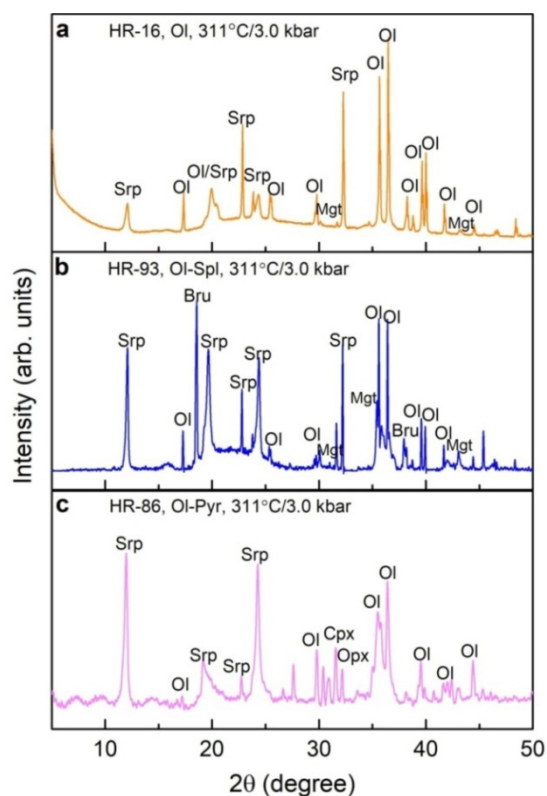


**Figure 1.** XRD patterns of typical experimental products of this study. (a) HR-16, 311 °C/3.0 kbar. Olivine (Ol) was taken as the starting reactant; (b) HR-93, 311 °C/3.0 kbar. A combination of olivine (Ol) and spinel (Spl) was used; (c) HR-86, 311 °C/3.0 kbar. Mechanical mixtures of olivine (Ol) and pyroxene minerals (Pyr) were used. Mgt: magnetite, Bru: brucite, Cpx: clinopyroxene, Srp: serpentine.

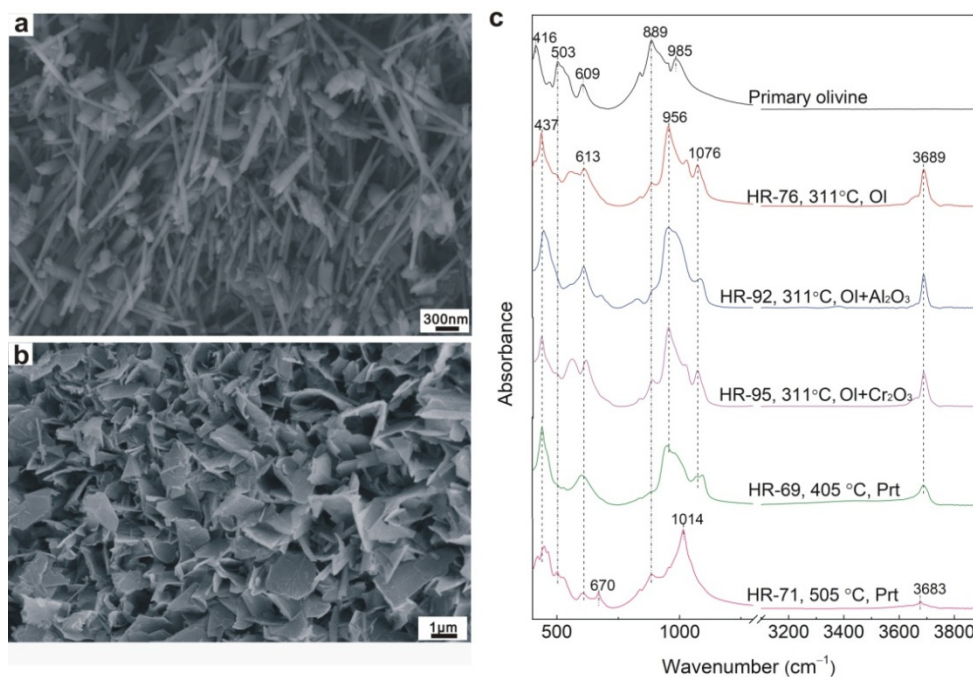
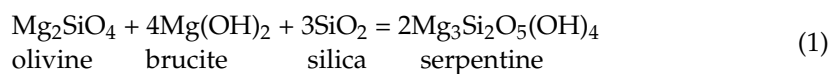


**Figure 2.** Identification of secondary hydrous minerals with scanning electron microscope imaging (a,b) and FTIR analyses (c).

In spite of the presence of brucite in many natural serpentinites [45,46], it was absent in all experiments at 400–500 °C and 3.0 kbar and in most experiments at 311 °C and 3.0 kbar, except those at 311 °C and 3.0 kbar with a combination of olivine and spinel (Figure 1). Experimental and thermodynamic simulations suggest that brucite formation during serpentinization can be affected by temperature, silica activity and chemical compositions of starting fluids [23,47]. First, thermodynamic models show that brucite production decreases significantly at temperatures of  $\geq 350$  °C, indicating that the stability of brucite may be reduced at higher temperatures [23]. Consistently, experimental studies show that brucite was formed during serpentinization at temperatures of  $\leq 300$  °C, and it was not found in experiments at higher temperatures (e.g., 350–500 °C) [21,22,30,31]. Moreover, brucite is not stable at high silica activity, under which conditions the reaction of brucite with silica results in the production of serpentine minerals [24,34,47].



As revealed by thermodynamic models, silica activity of peridotite serpentinization is around 1–2 orders of magnitude higher than that of olivine hydrothermal alteration [21]. As a consequence, brucite may not be stable in experiments with the presence of pyroxene. The absence of brucite during peridotite serpentinization was also reported by several previous experimental studies at temperatures of 300–500 °C and 3.0 kbar [24,35,48]. At relatively low temperatures (200–230 °C), brucite appeared only very late in the reaction (after 100 days) [31]. Additionally, analyses of natural serpentinites suggest that brucite tends to dissolve in seawater [49], and therefore brucite was not formed in experiments of this study with saline solutions (0.5 M NaCl).

### 3.2. Influence of Spinel and Pyroxene Minerals on Molecular Hydrogen ( $\text{H}_2$ ) Production

Blank experiments were carried out at 311–500 °C and 3.0 kbar, and solid reactants were loaded into gold capsules without any starting fluids. After 27 days, the concentrations of molecular hydrogen ( $\text{H}_2$ ) and hydrocarbons were below the limit of detection of gas chromatograph, indicating that olivine, pyroxene and spinel used in this study may not have any molecular hydrogen ( $\text{H}_2$ ) and hydrocarbons. Otherwise, elevated amounts of  $\text{H}_2$  and hydrocarbons (methane, ethane and propane) can be produced due to the decomposition of long-chain hydrocarbons [50]. This suggests that molecular hydrogen ( $\text{H}_2$ ) detected in the serpentinization experiments was produced during hydrothermal alteration of olivine.

The influence of spinel on molecular hydrogen ( $\text{H}_2$ ) during serpentinization was examined, and olivine, individually and in combinations with spinel, was reacted with saline solutions. In olivine experiments at 311 °C and 3.0 kbar, 80 mmol/kg  $\text{H}_2$  was produced after 27 days, which is around three times higher with the addition of spinel (Figure 3, Table 1). This suggests that spinel accelerates molecular hydrogen ( $\text{H}_2$ ) production during serpentinization.

Consistently, previous experiments showed a positive relationship between molecular hydrogen ( $\text{H}_2$ ) production and the amounts of spinel in starting reactants ( $R^2 = 0.97$ ), with higher  $\text{H}_2$  for experiments with more abundant spinel [25]. The influence of spinel has been proposed to result from the transfer of electrons to water adsorbed to the spinel surfaces, producing magnetite rinds around spinel [25]. Spinel in natural serpentinites is typically hydrothermally altered, leading to the formation of magnetite rinds [51–54]. The formation of Cr- and Al-depleted magnetite rinds indicates releases of aluminum (Al) and chromium (Cr) during hydrothermal alteration [35,51–54]. Aluminum and chromium accelerate the serpentinization of olivine [35,55], and they may impede the formation of iron oxide [48]. Therefore, Al and Cr may influence the production of  $\text{H}_2$  during hydrothermal alteration of olivine. In order to test such hypothesis, we carried out serpentinization experiments at 311 °C and 3.0 kbar with a combination of olivine and  $\text{Al}_2\text{O}_3$  or  $\text{Cr}_2\text{O}_3$  powders (Table 1), and molecular hydrogen ( $\text{H}_2$ ) production during the serpentinization of olivine becomes

around 2–3 times higher (Figure 3), suggesting that Al and Cr enhance molecular hydrogen ( $H_2$ ) production during olivine serpentinization. Therefore, the effect of spinel on molecular hydrogen ( $H_2$ ) production may result from releases of Al and Cr during hydrothermal alteration.

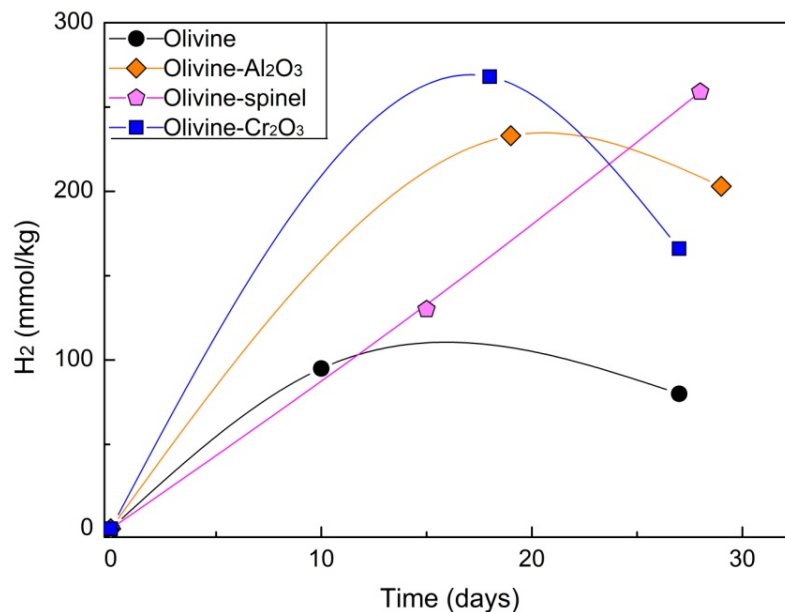


**Figure 3.** The concentrations of  $H_2$  in aqueous fluids (mmol/kg) for experiments at 311 °C and 3.0 kbar as a function of experimental durations (in day), showing that spinel, aluminum and chromium accelerate the production of  $H_2$  during serpentinization.

Aluminum and chromium promote the production of  $H_2$  during the serpentinization of olivine, which is closely associated with a dramatic increase in reaction rates. As suggested by previous experimental studies, aluminum and chromium speed up the serpentinization of olivine [35,55,56]. The progress of reaction in experiments with serpentine as the dominant hydrous phase was calibrated based on standard curves described in a previous study [35]. For experiments with serpentine and brucite as the dominant hydrous phases, the extent of reaction was calibrated according to a calibration curve based on infrared spectra of a combination of olivine, serpentine, and brucite with the percentage of olivine ranging from 10% to 48%. The proportions of serpentine have a positive correlation with  $\log(A_{441}/A_{503})$  ( $R^2 = 0.98$ ) (Figure 4a).  $A_{441}$  is the integrated infrared intensity of the vibration mode at  $441\text{ cm}^{-1}$ , and  $A_{503}$  is the integrated infrared intensity of the bending mode of Si-O band in olivine at  $503\text{ cm}^{-1}$ . Molecular hydrogen ( $H_2$ ) production has a positive correlation with the extent of reaction, with a higher extent of reaction for the production of more  $H_2$  (Figure 4b). Chromium slightly increases the rates of olivine hydrothermal alteration, and it has a pronounced effect on molecular hydrogen ( $H_2$ ) production (Figure 4b). In contrast, spinel not only enhances the hydrothermal alteration of olivine, but it also dramatically increases molecular hydrogen ( $H_2$ ) production. This also indicates that the dramatic increase in molecular hydrogen ( $H_2$ ) production with the addition of spinel is closely associated with aluminum and chromium rather than solely aluminum.

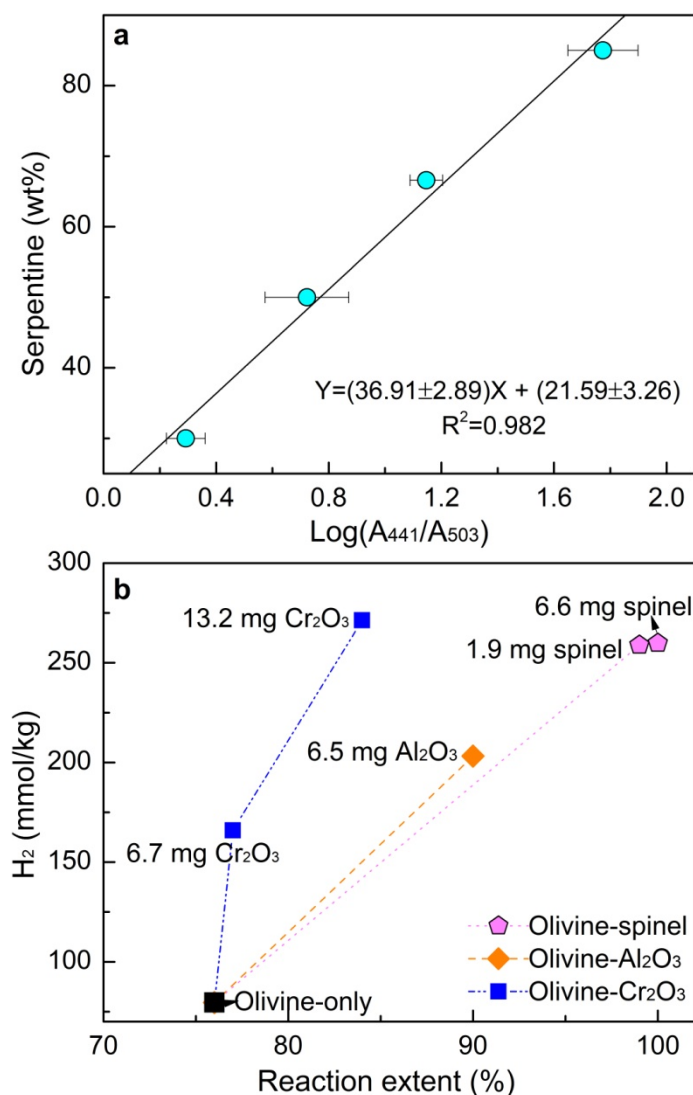


**Figure 4.** (a) Standard curves established to calibrate the proportions of serpentine in experiments of this study at 311 °C and 3.0 kbar, with serpentine and brucite as major hydrous minerals. (b) Positive correlation between the production of H<sub>2</sub> and the progress of reaction for experiments at 311 °C and 3.0 kbar, and the data correspond to experiments with a duration of 27–29 days.

Analyses of natural serpentinites show that their Al<sub>2</sub>O<sub>3</sub> is inversely correlated with SiO<sub>2</sub> contents [57], suggesting that Al<sup>3+</sup> substitutes for Si<sup>4+</sup> in tetrahedral sites of serpentine. The substitution of Al<sup>3+</sup> for Si in serpentine minerals is also observed for experiments of this study, which is indicated by the broadening of the Si-O infrared band at 956 cm<sup>-1</sup> (Figure 2). This suggests that aluminum is mobile during hydrothermal alteration of peridotite, and the mobility of Al is also indicated by chlorite formation in experiments with a combination of olivine and 13 wt% spinel or Al<sub>2</sub>O<sub>3</sub> (Figure 2). The incorporation of Al<sup>3+</sup> into serpentine results in a charge deficit, which may lead to the distribution of more Fe<sup>3+</sup> in octahedral sites of serpentine for compensation, and consequently the production of H<sub>2</sub> increases. Such hypothesis is supported by a decrease in the production of magnetite with the presence of Al<sub>2</sub>O<sub>3</sub> powders and the incorporation of more Fe into serpentine minerals [17,55]. The influence of Cr is possibly associated with the oxidation of Fe<sup>2+</sup> derived from olivine and pyroxene minerals by Cr<sup>6+</sup> as proposed previously [35].

Orthopyroxene taken in our experiments contains 4.14 wt% Al<sub>2</sub>O<sub>3</sub> and 0.40 wt% Cr<sub>2</sub>O<sub>3</sub>, and clinopyroxene has 6.04 wt% Al<sub>2</sub>O<sub>3</sub> and 1.04 wt% Cr<sub>2</sub>O<sub>3</sub>. Chemical compositions of natural serpentinized peridotites and experimental products after serpentinization suggest that pyroxene-derived serpentine has much less Al<sub>2</sub>O<sub>3</sub> than the Al<sub>2</sub>O<sub>3</sub> contents of pyroxene,

indicating that pyroxene leached some Al during serpentinization [35,36,58]. It has been estimated that ~50% of Al could be released from pyroxene [58]. The mobility of Cr is indicated by largely scattered Cr<sub>2</sub>O<sub>3</sub> contents of orthopyroxene-derived serpentine [35,58]. These observations indicate that pyroxene minerals may affect molecular hydrogen (H<sub>2</sub>) production during serpentinization.

The effect of pyroxene minerals on molecular hydrogen (H<sub>2</sub>) production was investigated by reacting a combination of olivine and pyroxene with saline solutions at 311 °C and 3.0 kbar. With the presence of pyroxene minerals, a sharp decline in molecular hydrogen (H<sub>2</sub>) production was observed, e.g., the concentrations of H<sub>2</sub> were 15 mmol/kg after 27 days, which are lower by more than one order of magnitude compared to H<sub>2</sub> produced in experiments with olivine. Therefore, pyroxene minerals impede molecular hydrogen (H<sub>2</sub>) production during serpentinization, in great contrast with spinel that promotes molecular hydrogen (H<sub>2</sub>) production.

Compared to olivine, pyroxene minerals have more abundant SiO<sub>2</sub>. Analyses of natural serpentinites and experimental products suggest that serpentine derived from pyroxene hydrothermal alteration contains smaller amounts of SiO<sub>2</sub> compared to the SiO<sub>2</sub> contents of pyroxene, which indicates releases of SiO<sub>2</sub> from pyroxene during hydrothermal alteration. Silica leached from pyroxene minerals participates in the reaction of olivine with H<sub>2</sub>O [36]. As indicated by thermodynamic models, silica significantly decreases H<sub>2</sub> production during olivine serpentinization [47,59]. The possibility that the formation of Si-rich surface layers inhibits the dissolution of olivine and pyroxene [25,43,60] and decreases the production of H<sub>2</sub>, however, is excluded. The absence of Si-rich surface layers is indicated by analyses of the experimental products with scanning electron microscopy and infrared spectroscopy.

### 3.3. Temperature Dependence of the Influence of Spinel and Pyroxene Minerals

Figure 5 shows that the effect of spinel and pyroxene on molecular hydrogen (H<sub>2</sub>) production during serpentinization is temperature dependent. The effect of pyroxene and spinel on molecular hydrogen (H<sub>2</sub>) production is most pronounced at 311 °C and 3.0 kbar, and it becomes much less significant at lower (200 °C/3.0 kbar) and higher temperatures (400–500 °C/3.0 kbar). Consistently, previous experiments showed that molecular hydrogen (H<sub>2</sub>) produced in olivine-experiments has no difference from H<sub>2</sub> formed in experiments with the presence of spinel [61]. At 400 °C and 3.0 kbar, a sharp decline in molecular hydrogen (H<sub>2</sub>) production was observed, e.g., H<sub>2</sub> in olivine-experiments decreased to 0.83 mmol/kg after 19 days (Table 1), which has the same trend as that observed for experiments with a combination of olivine and spinel/pyroxene. For experiments at 400–500 °C and 3.0 kbar with spinel-bearing peridotite (~60–65% olivine, 30–35% pyroxene and 1–2% spinel), molecular hydrogen (H<sub>2</sub>) production was slightly higher than H<sub>2</sub> formed in olivine-experiments (Figure 5), indicating that spinel combined with pyroxene minerals promotes the production of H<sub>2</sub> after olivine serpentinization.

Previous experiments suggest that molecular hydrogen (H<sub>2</sub>) production during serpentinization is directly linked to reaction rates [21,24,30]. The kinetics of olivine serpentinization increase greatly at higher temperatures, with a maximum value at ~300 °C [30,62,63]. With increasing temperatures (e.g., ≥350 °C), the kinetics of serpentinization are significantly slowed down [21,30,62]. Consistently, infrared spectra of the experimental products in this study at 300 °C and 3.0 kbar show a strong –OH band of serpentine and a weak Si–O band of olivine located at 505 cm<sup>−1</sup>; for experiments at 400–500 °C and 3.0 kbar, a strong Si–O band of olivine located at 505 cm<sup>−1</sup> and a weak –OH band of serpentine were observed (Figure 2), suggesting sluggish rates of reaction at 400–500 °C and 3.0 kbar. As a consequence, molecular hydrogen (H<sub>2</sub>) production decreases greatly at 400–500 °C and 3.0 kbar. Hydrothermal experiments suggest that pyroxene and spinel slightly enhance the serpentinization of olivine at 400–500 °C and 3.0 kbar, which is attributed to a decrease in Gibbs energy of olivine serpentinization with the presence of silica released from pyroxene

minerals [36]. This may consequently increase molecular hydrogen ( $H_2$ ) production during serpentinization.

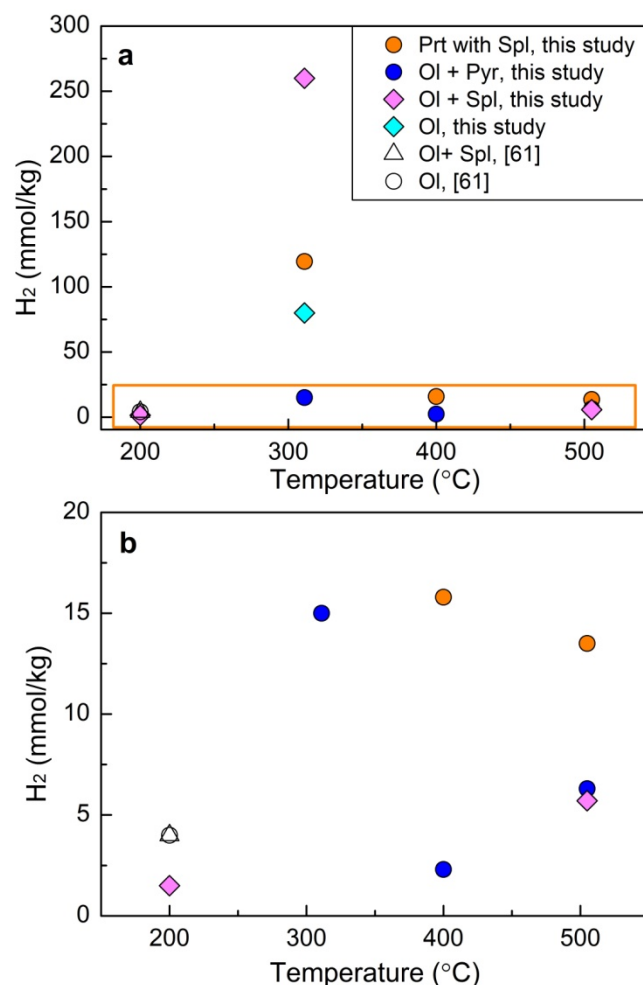


**Figure 5.** (a) Temperature dependence of the influence of spinel and pyroxene minerals on  $H_2$  production during serpentinization. (b) An enlargement of the yellow rectangle in (a). Ol: olivine, Pyr: pyroxene, Spl: spinel, Prt: peridotite.

Temperature dependence of  $H_2$  production after olivine serpentinization may reflect distinct mineralogical assemblages of the experimental products at lower (e.g., 200–300 °C and 3.0 kbar) and higher temperatures (e.g., 400–500 °C and 3.0 kbar). Scanning electron microscope imaging and FTIR analyses have revealed that fibrous chrysotile was the main secondary hydrous mineral for most experiments at 311 °C and 3.0 kbar. The dominant hydrous phase in experiments at 400 °C and 3.0 kbar was lizardite, and lizardite and talc were generated at 500 °C and 3.0 kbar. Talc formation indicates that silica activity may be higher than that of experiments with serpentine [21]. The increase in silica activity at higher temperatures may lead to a decline in molecular hydrogen ( $H_2$ ) production [59].

### 3.4. Comparison of $H_2$ Production in This Study with That from Previous Studies

Chromite, an accessory mineral of ultramafic rocks, is commonly present in serpentinization experiments [24,25,35,36,61,64]. Only a few studies have reported that chromite greatly accelerates molecular hydrogen ( $H_2$ ) production during serpentinization [25], and most studies have proposed a negligible influence of chromite [24,61,64]. Experiments of Mayhew et al. [25] were conducted at relatively low temperatures, 55–100 °C, with an experimental duration up to 100 days, and they showed that chromite enhanced molecular hydrogen ( $H_2$ ) production by around three times. In contrast, the influence of chromi-

teon H<sub>2</sub> production was found to be negligible, based on short-period experiments (40 days) at 200 °C and 200 bar with and without the addition of 1 wt% chromite [61]. The discrepancy may be attributed to the production of lower molecular hydrogen (H<sub>2</sub>) due to relatively shorter periods [61], which may obscure the influence of chromite. Consistently, for experiments of this study at 200 °C and 3.0 kbar with a combination of olivine and 22% spinel, molecular hydrogen (H<sub>2</sub>) produced after 13 days was notably similar to H<sub>2</sub> formed in olivine-only experiments (Table 1). Experiments of Lazar et al. [64] were performed at 300 °C and 350 bar, and they showed that the serpentinization of komatiite with the presence of chromite produced similar amounts of H<sub>2</sub> as that formed during komatiite hydrothermal alteration (Table 2). The contrast between experimental results of Lazar et al. [64] from this study may result from the presence of glass, Cu-Zn alloys and sulfides in komatiite, which may influence the formation of H<sub>2</sub>.

**Table 2.** The production of H<sub>2</sub> in previous experimental studies.

T (°C)	P (bar)	Solid Reactant	Starting Fluids	W/R Ratios	Time (Days)	H <sub>2</sub> (mmol/kg)	References
300	500	Ol	NaCl	2.25	69	158	[19]
200	500	Prt	seawater	1.1	328	77	[22]
200	300	Ol	seawater + NaHCO <sub>3</sub>	2.5	33	2	[33]
300	300	Prt	H <sub>2</sub> O	0.67	70	76	[24]
200	200	Ol + Chr <sup>a</sup>	H <sub>2</sub> O	2.5	21	4	[61]
200	200	Ol	H <sub>2</sub> O	2.5	21	4	[61]
300	350	Koma	H <sub>2</sub> O	3.7	63	74	[64]
300	350	Koma + Chr	H <sub>2</sub> O	4.7	63	55	[64]
300	500	Ol	NaCl	2.1	111	11	[30]
200	500	Ol	NaCl	1.8	138	0.09	[30]
400	500	Ol	NaCl + MgCl <sub>2</sub>	4.0	64	1.2	[21]
400	500	Prt <sup>b</sup>	NaCl + MgCl <sub>2</sub>	4.0	60	6.8	[21]

Ol: olivine, Prt: peridotite, Chr: chromite, Koma: komatiite. <sup>a</sup> The starting material is olivine and 1 wt% chromite. <sup>b</sup> The starting material is 76% olivine, 17% orthopyroxene, and 7% clinopyroxene.

Hydrothermal experiments of Shibuya et al. [17] were conducted at 300 °C and 500 bar using two types of komatiites that have essentially the same chemical compositions except Al<sub>2</sub>O<sub>3</sub> contents, 5% and 10%, respectively. It was revealed that H<sub>2</sub> production in the experiment with 5% Al<sub>2</sub>O<sub>3</sub> is higher than that with 10% Al<sub>2</sub>O<sub>3</sub>, which suggests that aluminum impedes the production of H<sub>2</sub> during hydrothermal alteration of komatiite [17]. The discrepancy from experimental findings of this study may result from different starting reactants. Komatiite is composed of olivine, glass, and minor chromite, and it contains more abundant SiO<sub>2</sub> compared to olivine [17]. Hydrothermal alteration of komatiite could release more SiO<sub>2</sub> into aqueous fluids compared to that after hydrothermal alteration of olivine [19,65,66], which suggests that the serpentinization of olivine is distinct from the hydrothermal alteration of komatiite.

Peridotites or mixtures of olivine and orthopyroxene have been used as starting reactants in serpentinization experiments [21,22,24,31]. At relatively low temperatures (230 °C), orthopyroxene was found to have a negligible influence on molecular hydrogen (H<sub>2</sub>) production during the serpentinization of olivine, and it enhanced molecular hydrogen (H<sub>2</sub>) production after very long periods (e.g., 386 days), which is associated with a dramatic increase in pH [31]. The discrepancy from experimental results of this study may be attributed to the different experimental conditions, which include relatively low temperatures (230 °C), the production of brucite and a dramatic increase in pH [31]. The kinetics of orthopyroxene serpentinization under these conditions are 2–3 times faster than the rates of olivine hydrothermal alteration [31], which is distinct from the serpentinization of peridotite at 311 °C and 3.0 kbar with slower rates of pyroxene serpentinization at reaction extent of ≤70% [35]. With increasing temperatures (400 °C), the serpentinization of olivine

produced the same amounts of molecular hydrogen ( $H_2$ ) as  $H_2$  formed in experiments with a combination of olivine and pyroxene minerals [21]. This indicates a negligible influence of pyroxene minerals on molecular hydrogen ( $H_2$ ) production at higher temperatures, which agrees well with experimental results of this study.

### 3.5. Geological Implications

This study shows that spinel and pyroxene strongly influence the production of  $H_2$  during hydrothermal alteration of olivine, which is connected with the mobility of Al, Cr and silica. Analyses of natural serpentinite suggest that they contain abundant  $Al_2O_3$ , ranging from <1 wt% to >20 wt% [46,58]. Although the solubility of  $Al_2O_3$  in aqueous fluids is very low, <100 ppm [67], the mobility of Al during serpentinization is supported by the following geological evidence: (1) occurrences of aluminum hydroxide in serpentinites [68], (2) the formation of pyroxene-derived serpentine with less  $Al_2O_3$  compared to that of primary pyroxene [46,57,58], and (3) the production of ferrichromite and magnetite rinds around primary spinel [54,58,69]. Olivine in natural geological settings is intimately associated with minerals with abundant  $Al_2O_3$ , such as pyroxene, plagioclase, and spinel, which could release some of their Al during hydrothermal alteration of ultramafic rocks, and consequently the production of  $H_2$  can be enhanced.

Fluids circulating serpentinizing peridotites commonly contain abundant  $SiO_2$  [5]. Analyses of natural serpentinites show that serpentine minerals derived from the hydrothermal alteration of pyroxene typically have smaller amounts of  $SiO_2$  compared to the  $SiO_2$  contents of pyroxene [35,48,57,58], indicating that pyroxene minerals leached some of their  $SiO_2$  during hydrothermal alteration. The mobility of silica during hydrothermal alteration of ultramafic rocks is also indicated by the replacement of plagioclase by various Si-poor silicates, such as grossular, wollastonite and zoisite [68]. Experimental and thermodynamic studies have revealed that silica impedes the oxidation of  $Fe^{2+}$  derived from olivine and pyroxene into  $Fe^{3+}$  [47], which may consequently reduce molecular hydrogen ( $H_2$ ) production during serpentinization.

The experimental results of this study may have important implications for  $H_2$  production during serpentinization. Molecular hydrogen can feed communities of microorganisms in serpentinite-hosted settings such as deep-sea hydrothermal vents, alkaline springs, and the deep subsurface [8–12]. The microorganisms can endure high temperature (e.g., ~100 °C), high pressure, and extremely acidic or alkaline conditions. This may be an analog for the genesis of life in the Hadean ocean. Geological studies suggest that life has been present on Earth for at least 3.5 Gyr, and it probably began before 3.8 Gyr [70]. Biological studies indicate that the ancestor of life is hyperthermophile, i.e., the organism that lives at temperatures of 80–110 °C or more [71]. Therefore, serpentinization may therefore be favorable for the origin and evolution of life [72,73]. There should be some critical steps for the early Earth to evolve from a magma ocean to a habitable planet in the Hadean eon. Ultramafic rocks may be widely exposed on the surface of the early Earth, and the atmosphere is mainly composed of  $H_2O$  and  $CO_2$  [71,74]. Interactions between ultramafic rocks and  $H_2O$  in early atmosphere may significantly change the physicochemical condition of the Earth's surface and initiate the prebiotic chemical conditions for life genesis.

## 4. Conclusions

The effect of pyroxene and spinel on molecular hydrogen ( $H_2$ ) generation during the serpentinization of olivine was experimentally studied at 311–500 °C and 3.0 kbar, where olivine, individually or in combined with pyroxene and spinel, was reacted with saline solutions (0.5 M NaCl). At 311 °C and 3.0 kbar, spinel was found to accelerate  $H_2$  generation by around 2–3 times, and the increase in  $H_2$  generation is directly linked to releases of aluminum and chromium during hydrothermal alteration. Aluminum and chromium significantly enhance molecular hydrogen ( $H_2$ ) generation during olivine serpentinization, which was confirmed by serpentinization experiments conducted at 311 °C and 3.0 kbar with the presence of  $Al_2O_3$  and  $Cr_2O_3$  powders. In spite of releases of aluminum and

chromium from pyroxene minerals, pyroxene minerals greatly inhibit H<sub>2</sub> generation during serpentinization, which may result from releases of silica from pyroxene minerals. The influence of pyroxene minerals and spinel on H<sub>2</sub> generation is temperature dependent, and it becomes negligible at lower temperatures (200 °C and 3.0 kbar). At higher temperatures (400–500 °C and 3.0 kbar), the addition of the combination of pyroxene and spinel slightly increases H<sub>2</sub> generation during olivine serpentinization, and the presence of individual pyroxene or spinel has a negligible effect. Olivine in natural geological settings is commonly associated with aluminum-rich minerals (e.g., pyroxene, spinel and plagioclase), and therefore H<sub>2</sub> generation can be greatly affected.

**Author Contributions:** R.H. conceived of the primary data, conducted all the experiments, analyzed most samples and wrote the manuscript. W.S. and X.S. co-write the manuscript. X.D., X.S. analyzed some samples. All authors have read and agreed to the published version of the manuscript.

**Funding:** This work was financially supported by the Natural Science Foundation of China (41873069), the Strategic Priority Research Program of the Chinese Academy of Sciences (XDA22050103), and the National Key R&D Program of China (2016YFC0600408).

**Data Availability Statement:** The data presented in this study are available within the article.

**Acknowledgments:** We thank J. H. Zhu from the Second Institute of Oceanography, State Oceanic Administration of China for performing scanning electron microscope imaging. We would like to express our gratitude to S. Jiang from South China University of Technology for the assistance during FTIR analyses.

**Conflicts of Interest:** The authors declare that there are no conflict of interest regarding the publication of this paper.

## References

1. Carlson, R.L. The abundance of ultramafic rocks in Atlantic Ocean crust. *Geophys. J. Int.* **2001**, *144*, 37–48. [[CrossRef](#)]
2. Carlson, R.L.; Miller, D.J. Mantle wedge water contents estimated from seismic velocities in partially serpentinized peridotites. *Geophys. Res. Lett.* **2003**, *30*, 1250. [[CrossRef](#)]
3. Hirth, G.; Guillot, S. Rheology and tectonic significance of serpentinite. *Elements* **2013**, *9*, 107–113. [[CrossRef](#)]
4. Charlou, J.L.; Fouquet, Y.; Bougault, H.; Donval, J.P.; Etoubleau, J.; Jean-Baptiste, P.; Dapoigny, A.; Appriou, P.; Rona, P.A. Intense CH<sub>4</sub> plumes generated by serpentinization of ultramafic rocks at the intersection of the 15°20'N fracture zone and the Mid-Atlantic Ridge. *Geochim. Cosmochim. Acta* **1998**, *62*, 2323–2333. [[CrossRef](#)]
5. Charlou, J.L.; Donval, J.P.; Douville, E.; Jean-Baptiste, P.; Radford-Knoery, J.; Fouquet, Y.; Dapoigny, A.; Stievenard, M. Compared geochemical signatures and the evolution of Menez Gwen (37°50' N) and Lucky Strike (37°17' N) hydrothermal fluids, south of the Azores triple junction on the Mid-Atlantic Ridge. *Chem. Geol.* **2000**, *171*, 49–75. [[CrossRef](#)]
6. Charlou, J.L.; Donval, J.P.; Fouquet, Y.; Jean-Baptiste, P.; Holm, N. Geochemistry of high H<sub>2</sub> and CH<sub>4</sub> vent fluids issuing from ultramafic rocks at the Rainbow hydrothermal field (36°14' N, MAR). *Chem. Geol.* **2002**, *191*, 345–359. [[CrossRef](#)]
7. Kelley, D.S.; Karson, J.A.; Blackman, D.K.; Früh-Green, G.L.; Butterfield, D.A.; Lilley, M.D.; Olson, E.J.; Schrenk, M.O.; Roe, K.K.; Lebon, G.T.; et al. An off-axis hydrothermal vent field near the Mid-Atlantic Ridge at 30° N. *Nature* **2001**, *412*, 145–149. [[CrossRef](#)]
8. Brazelton, W.J.; Schrenk, M.O.; Kelley, D.S.; Baross, J.A. Methane- and sulfur-metabolizing microbial communities dominate the Lost City hydrothermal field ecosystem. *Appl. Environ. Microbiol.* **2006**, *72*, 6257–6270. [[CrossRef](#)]
9. Brazelton, W.J.; Nelson, B.; Schrenk, M.O. Metagenomic evidence for H<sub>2</sub> oxidation and H<sub>2</sub> production by serpentinite-hosted subsurface microbial communities. *Front. Microbiol.* **2010**, *2*, 1–16. [[CrossRef](#)]
10. McCollom, T.M.; Seewald, J.S. Serpentinites, hydrogen, and life. *Elements* **2013**, *9*, 129–134. [[CrossRef](#)]
11. Schrenk, M.O.; Kelley, D.S.; Bolton, S.A.; Baross, J.A. Low archaeal diversity linked to seafloor geochemical processes at the Lost City Hydrothermal Field, Mid-Atlantic Ridge. *Environ. Microbiol.* **2004**, *6*, 1086–1095. [[CrossRef](#)] [[PubMed](#)]
12. Schrenk, M.O.; Brazelton, W.J.; Lang, S.Q. Serpentinization, carbon, and deep life. *Rev. Mineral. Geochem.* **2013**, *75*, 575–606. [[CrossRef](#)]
13. Takai, K.; Nakamura, K.; Suzuki, K.; Inagaki, F.; Nealson, K.H.; Kumagai, H. Ultramafics-hydrothermalism-hydrogenesis-hyperSLiME (UltraH<sup>3</sup>) linkage: A key insight into early microbial ecosystem in the Archean deep-sea hydrothermal systems. *Paleontol. Res.* **2006**, *10*, 269–282. [[CrossRef](#)]
14. Yoshizaki, M.; Shibuya, T.; Suzuki, K.; Shimizu, K.; Nakamura, K.; Takai, K.; Omori, S.; Maruyama, S. H<sub>2</sub> generation by experimental hydrothermal alteration of komatiitic glass at 300 °C and 500 bars: A preliminary result from on-going experiment. *Geochem. J.* **2009**, *43*, e17–e22. [[CrossRef](#)]
15. Russell, M.J.; Hall, A.J.; Martin, W. Serpentinization as a source of energy at the origin of life. *Geobiology* **2010**, *8*, 355–371. [[CrossRef](#)]

16. Shibuya, T.; Komiya, T.; Nakamura, K.; Takai, K.; Maruyama, S. Highly alkaline, high-temperature hydrothermal fluids in the early Archean ocean. *Precambrian. Res.* **2010**, *182*, 230–238. [[CrossRef](#)]
17. Shibuya, T.; Yoshizaki, M.; Sato, M.; Shimizu, K.; Nakamura, K.; Omori, S.; Suzuki, K.; Takai, K.; Tsunakawa, H.; Maruyama, S. Hydrogen-rich hydrothermal environments in the Hadean ocean inferred from serpentinization of komatiites at 300 °C and 500 bar. *Prog. Earth Planet. Sci.* **2015**, *2*. [[CrossRef](#)]
18. Song, S.G.; Su, L.; Niu, Y.L.; Lai, Y.; Zhang, L.F. CH<sub>4</sub> inclusions in orogenic harzburgite: Evidence for reduced slab fluids and implication for redox melting in mantle wedge. *Geochim. Cosmochim. Acta* **2009**, *73*, 1737–1754. [[CrossRef](#)]
19. Berndt, M.E.; Allen, D.E.; Seyfried, W.E., Jr. Reduction of CO<sub>2</sub> during serpentinization of olivine at 300 °C and 500 bar. *Geology* **1996**, *24*, 351–354. [[CrossRef](#)]
20. McCollom, T.M.; Seewald, J.S. A reassessment of the potential for reduction of dissolved CO<sub>2</sub> to hydrocarbons during serpentinization of olivine. *Geochim. Cosmochim. Acta* **2001**, *65*, 3769–3778. [[CrossRef](#)]
21. Allen, D.E.; Seyfried, W.E., Jr. Compositional controls on vent fluids from ultramafic-hosted hydrothermal systems at mid-ocean ridges: An experimental study at 400 °C, 500 bars. *Geochim. Cosmochim. Acta* **2003**, *67*, 1531–1542. [[CrossRef](#)]
22. Seyfried, W.E., Jr.; Foustoukos, D.I.; Fu, Q. Redox evolution and mass transfer during serpentinization: An experimental and theoretical study at 200 °C, 500 bar with implications for ultramafic-hosted hydrothermal systems at mid-ocean ridges. *Geochim. Cosmochim. Acta* **2007**, *71*, 3872–3886. [[CrossRef](#)]
23. McCollom, T.M.; Bach, W. Thermodynamic constraints on hydrogen generation during serpentinization of ultramafic rocks. *Geochim. Cosmochim. Acta* **2009**, *73*, 856–875. [[CrossRef](#)]
24. Marcaillou, C.; Muñoz, M.; Vidal, O.; Parra, T.; Harfouche, M. Mineralogical evidence for H<sub>2</sub> degassing during serpentinization at 300 °C/300 bar. *Earth Planet. Sci. Lett.* **2011**, *303*, 281–290. [[CrossRef](#)]
25. Mayhew, L.E.; Ellison, E.T.; McCollom, T.M.; Trainor, T.P.; Templeton, A.S. Hydrogen generation from low-temperature water-rock interactions. *Nat. Geosci.* **2013**, *6*. [[CrossRef](#)]
26. Huang, R.F.; Sun, W.D.; Ding, X.; Liu, J.Z.; Peng, S.B. Olivine versus peridotite during serpentinization: Gas formation. *Sci. China Earth Sci.* **2015**, *58*, 2165–2174. [[CrossRef](#)]
27. Huang, R.F.; Sun, W.D.; Ding, X.; Liu, J.Q.; Zhan, W.H. Formation of hydrogen gas and alkane during peridotite serpentinization. *Acta Petrol. Sin.* **2015**, *31*, 1901–1907.
28. Huang, R.F.; Sun, W.D.; Liu, J.Z.; Ding, X.; Peng, S.B.; Zhan, W.H. The H<sub>2</sub>/CH<sub>4</sub> ratio during serpentinization cannot reliably identify biological signatures. *Sci. Rep.* **2016**, *6*, 33821. [[CrossRef](#)]
29. Huang, R.F.; Sun, W.D.; Song, M.S.; Ding, X. Influence of pH on molecular hydrogen (H<sub>2</sub>) generation and reaction rates during serpentinization of peridotite and olivine. *Minerals* **2019**, *9*, 661. [[CrossRef](#)]
30. McCollom, T.M.; Klein, F.; Robbins, M.; Moskowitz, B.; Berquó, T.S.; Jöns, N.; Bach, W.; Templeton, A. Temperature trends for reaction rates, hydrogen generation, and partitioning of iron during experimental serpentinization of olivine. *Geochim. Cosmochim. Acta* **2016**, *181*, 175–200. [[CrossRef](#)]
31. McCollom, T.M.; Klein, F.; Moskowitz, B.; Berquó, T.S.; Bach, W.; Templeton, A.S. Hydrogen generation and iron partitioning during experimental serpentinization of an olivine-pyroxene mixture. *Geochim. Cosmochim. Acta* **2020**, *282*, 55–75. [[CrossRef](#)]
32. Lamadrid, H.M.; Rimstidt, J.D.; Schwarzenbach, E.M.; Klein, F.; Ulrich, S.; Dolocan, A.; Bodnar, R.J. Effect of water activity on rates of serpentinization of olivine. *Nat. Commun.* **2017**, *8*, 16107. [[CrossRef](#)]
33. Jones, L.C.; Rosenbauer, R.; Goldmith, J.I.; Oze, C. Carbonate control of H<sub>2</sub> and CH<sub>4</sub> production in serpentinization systems at elevated P-Ts. *Geophys. Res. Lett.* **2010**, *37*, L14306. [[CrossRef](#)]
34. Syverson, D.D.; Tutolo, B.M.; Borrok, D.M.; Seyfried, W.E., Jr. Serpentinization of olivine at 300 °C and 500 bars: An experimental study examining the role of silica on the reaction path and oxidation state of iron. *Chem. Geol.* **2017**, *475*, 122–134. [[CrossRef](#)]
35. Huang, R.F.; Song, M.S.; Ding, X.; Zhu, S.Y.; Zhan, W.H.; Sun, W.D. Influence of pyroxene and spinel on the kinetics of peridotite serpentinization. *J. Geophys. Res.* **2017**, *122*. [[CrossRef](#)]
36. Huang, R.F.; Sun, W.D.; Ding, X.; Zhao, Y.S.; Song, M.S. Effect of pressure on the kinetics of peridotite serpentinization. *Phys. Chem. Miner.* **2020**, *47*, 33. [[CrossRef](#)]
37. Chen, D.G.; Li, B.X.; Zhi, X.C. Genetic geochemistry of mantle-derived peridotite xenolith from Panshishan, Jiangsu. *Geochimica* **1994**, *23*, 13–24.
38. Sun, W.D.; Peng, Z.C.; Zhi, X.C.; Chen, D.G.; Wang, Z.R.; Zhou, X.H. Osmium isotope determination on mantle-derived peridotite xenoliths from Panshishan with N-TIMS. *Chinese Sci. Bull.* **1998**, *43*, 573–575. [[CrossRef](#)]
39. Xu, X.S.; Griffin, W.L.; O'Reilly, S.Y.; Pearson, N.J.; Geng, H.Y.; Zheng, J.P. Re-Os isotopes of sulfides in mantle xenoliths from eastern China: Progressive modification of lithospheric mantle. *Lithos* **2008**, *102*, 43–64. [[CrossRef](#)]
40. Xiong, Y.Q.; Geng, A.S.; Wang, Y.P.; Liu, D.H.; Jia, R.F.; Shen, J.G. Kinetic simulating experiment on the secondary hydrocarbon generation of kerogen. *Sci. China Ser. D-Earth Sci.* **2001**, *45*, 13–20. [[CrossRef](#)]
41. Pan, C.C.; Yu, L.P.; Liu, J.Z.; Fu, J.M. Chemical and carbon isotopic fractionations of gaseous hydrocarbons during abiogenic oxidation. *Earth Planet. Sci. Lett.* **2006**, *246*, 70–89. [[CrossRef](#)]
42. Lafay, R.; Montes-Hernandez, G.; Janots, E.; Chiriac, R.; Findling, N.; Toche, F. Mineral replacement rate of olivine by chrysotile and brucite under high alkaline conditions. *J. Cryst. Growth* **2012**, *347*, 62–72. [[CrossRef](#)]
43. Lafay, R.; Montes-Hernandez, G.; Janots, E.; Chiriac, R.; Findling, N.; Toche, F. Simultaneous precipitation of magnesite and lizardite from hydrothermal alteration of olivine under high-carbonate alkalinity. *Chem. Geol.* **2014**, *368*, 63–75. [[CrossRef](#)]

44. Liu, X.W.; Liu, X.X.; Hu, Y.H. Investigation of the thermal decomposition of talc. *Clay Clay Miner.* **2014**, *62*, 137–144. [[CrossRef](#)]
45. Bach, W.; Paulick, H.; Garrido, C.J.; Ildefonse, B.; Meurer, W.P.; Humphris, S.E. Unraveling the sequence of serpentinization reactions: Petrology, mineral chemistry, and petrophysics of serpentinites from MAR 15 °N (ODP Leg 209, Site 1274). *Geophys. Res. Lett.* **2006**, *33*, L13306. [[CrossRef](#)]
46. Beard, J.S.; Frost, B.R.; Fryer, P.; McCaig, A.; Searle, R.; Ildefonse, B.; Zinin, P.; Sharma, S.K. Onset and progression of serpentinization and magnetite formation in olivine-rich troctolite from IODP Hole U1309D. *J. Petrol.* **2009**, *50*, 387–403. [[CrossRef](#)]
47. Frost, B.R.; Beard, J.S. On silica activity and serpentinization. *J. Petrol.* **2007**, *48*, 1351–1368. [[CrossRef](#)]
48. Huang, R.F.; Lin, Q.T.; Sun, W.D.; Ding, X.; Zhan, W.H.; Zhu, J.H. The production of iron oxide during peridotite serpentinization: Influence of pyroxene. *Geosci. Front.* **2017**, *8*, 1311–1321. [[CrossRef](#)]
49. Jöns, N.; Kahl, W.A.; Bach, W. Reaction-induced porosity and onset of low-temperature carbonation in abyssal peridotites: Insights from 3D high-resolution microtomography. *Lithos* **2017**, *268–271*, 274–284. [[CrossRef](#)]
50. Tingle, T.N.; Hochella, M.F., Jr.; Becker, C.H.; Malhotra, R. Organic compounds on crack surfaces in olivine from San Carlos, Arizona, and Hualalai Volcano, Hawaii. *Geochim. Cosmochim. Acta* **1990**, *54*, 477–485. [[CrossRef](#)]
51. Beeson, M.H.; Jackson, E.D. Chemical composition of altered chromites from the Stillwater Complex, Montana. *Am. Mineral.* **1969**, *54*, 1084–1100.
52. Hamlyn, P.R. Chromite alteration in the Panton Sill, East Kimberley Region, Western Australia. *Mineral. Mag.* **1975**, *40*, 181–192. [[CrossRef](#)]
53. Burkhard, D.J.M. Accessory chromium spinels: Their coexistence and alteration in serpentinites. *Geochim. Cosmochim. Acta* **1993**, *57*, 1297–1306. [[CrossRef](#)]
54. Mellini, M.; Rumori, C.; Viti, C. Hydrothermally reset magmatic spinels in retrograde serpentinites: Formation of “ferritchromit” rims and chlorite aureoles. *Contrib. Mineral. Petr.* **2005**, *149*, 266–275. [[CrossRef](#)]
55. Andreani, M.; Daniel, I.; Pollet-Villard, M. Aluminum speeds up the hydrothermal alteration of olivine. *Am. Mineral.* **2013**, *98*, 1738–1744. [[CrossRef](#)]
56. Pens, M.; Andreani, M.; Daniel, I.; Perrillat, J.P.; Cardon, H. Contrasted effect of aluminum on the serpentinization rate of olivine and orthopyroxene under hydrothermal conditions. *Chem. Geol.* **2016**, *441*, 256–264. [[CrossRef](#)]
57. Bonifacie, M.; Busigny, V.; Mével, C.; Philippot, P.; Agrinier, P.; Jendrzewski, N.; Scambelluri, M.; Javoy, M. Chlorine isotopic composition in seafloor serpentinites and high-pressure metaperidotites. Insights into oceanic serpentinization and subduction processes. *Geochim. Cosmochim. Acta* **2008**, *72*, 126–139. [[CrossRef](#)]
58. Dungan, M.A. A microprobe study of antigorite and some serpentine pseudomorphs. *Can. Mineral.* **1979**, *17*, 771–784.
59. Seyfried, W.E., Jr.; Pester, N.J.; Ding, K.; Rough, M. Vent fluid chemistry of the Rainbow hydrothermal system (36° N, MAR): Phase equilibria and in situ pH controls on seafloor alteration processes. *Geochim. Cosmochim. Acta* **2011**, *75*, 1574–1593. [[CrossRef](#)]
60. Béarat, H.; Mckelvy, M.J.; Chizmeshya, A.V.G.; Gormley, D.; Nunez, R.; Carpenter, R.W.; Squires, K.; Wolf, G.H. Carbon sequestration via aqueous olivine mineral carbonation: Role of passivating layer formation. *Environ. Sci. Technol.* **2006**, *40*, 4802–4808. [[CrossRef](#)]
61. Oze, C.; Jones, L.C.; Goldsmith, J.I.; Rosenbauer, R.J. Differentiating biotic from abiotic methane genesis in hydrothermally active planetary surfaces. *Proc. Natl. Acad. Sci. USA* **2012**, *109*, 9750–9754. [[CrossRef](#)]
62. Martin, B.; Fyfe, W.S. Some experimental and theoretical observations on the kinetics of hydration reactions with particular reference to serpentinization. *Chem. Geol.* **1970**, *6*, 185–202. [[CrossRef](#)]
63. Wegner, W.W.; Ernst, W.G. Experimentally determined hydration and dehydration reaction rates in the system MgO-SiO<sub>2</sub>-H<sub>2</sub>O. *Am. J. Sci.* **1983**, *283*, 151–180.
64. Lazar, C.; McCollom, T.M.; Manning, C.E. Abiogenic methanogenesis during experimental komatiite serpentinization: Implications for the evolution of the early Precambrian atmosphere. *Chem. Geol.* **2012**, *326–327*, 102–112. [[CrossRef](#)]
65. Okamoto, A.; Ogasawara, Y.; Ogawa, Y.; Tsuchiya, N. Progress of hydration reactions in olivine-H<sub>2</sub>O and orthopyroxene-H<sub>2</sub>O systems at 250 °C and vapor-saturated pressure. *Chem. Geol.* **2011**, *289*, 245–255. [[CrossRef](#)]
66. Ueda, H.; Shibuya, T.; Sawaki, Y.; Saitoh, M.; Takai, K.; Maruyama, S. Reactions between komatiite and CO<sub>2</sub>-rich seawater at 250 and 350 °C, 500 bars: Implications for hydrogen generation in the Hadean seafloor hydrothermal system. *Prog. Earth Planet. Sci.* **2016**, *3*. [[CrossRef](#)]
67. Manning, C.E. Solubility of corundum + kyanite in H<sub>2</sub>O at 700 °C and 10 kbar: Evidence for Al-Si complexing at high pressure and temperature. *Geofluids* **2007**, *7*, 258–269. [[CrossRef](#)]
68. Beard, J.; Hopkinson, L. A fossil, serpentinization-related hydrothermal vent, Ocean Drilling Program Leg 173, Site 1068 (Iberia Abyssal Plain): Some aspects of mineral and fluid chemistry. *J. Geophys. Res.* **2000**, *105*, 16527–16539. [[CrossRef](#)]
69. Hébert, R.; Adamson, A.C.; Komor, S.C. Metamorphic petrology of ODP Leg 109, Hole 670A serpentinized peridotites: Serpentinization processes at a slow spreading ridge environment. In Proceedings of the Ocean Drilling Program, Scientific Results 106/109, Ocean Drilling Program, College Station, TX, USA; 1990; pp. 103–115. [[CrossRef](#)]
70. Nisbet, E.G.; Fowler, C.M.R. Some liked it hot. *Nature* **1996**, *382*, 404–405. [[CrossRef](#)]
71. Sleep, N.H. The Hadean-Archaeon environment. *Cold Spring Harb. Perspect. Biol.* **2010**, *2*, a002527. [[CrossRef](#)]
72. Holm, N.G.; Andersson, E.M. Abiotic synthesis of organic compounds under the conditions of submarine hydrothermal systems: A perspective. *Planet. Space Sci.* **1995**, *43*, 153–159. [[CrossRef](#)]

- 
73. Sleep, N.H.; Meibom, A.; Fridriksson, T.; Coleman, R.G.; Bird, D.K. H<sub>2</sub>-rich fluids from serpentinization: Geochemical and biotic implications. *Proc. Natl. Acad. Sci. USA* **2004**, *101*, 12818–12823. [[CrossRef](#)] [[PubMed](#)]
  74. Zahnle, K.; Arndt, N.; Cockell, C.; Halliday, A.; Nisbet, E.; Selsis, F.; Sleep, N.H. Emergence of a habitable planet. *Space Sci. Rev.* **2007**, *129*, 35–78. [[CrossRef](#)]